

Modeling the chronologies and size distributions of Ceres and Vesta craters

F. ROIG¹ AND D. NESVORNÝ²

¹*Observatório Nacional*

Rua Gal José Cristino 77, Rio de Janeiro, RJ 20921-400, Brazil

²*Southwest Research Institute*

1050 Walnut St., Boulder, CO 80302, USA

(Received 16-Jan-2020; Revised 29-May-2020; Accepted 16-Jul-2020)

Submitted to AJ

Abstract

We infer the crater chronologies of Ceres and Vesta from a self-consistent dynamical model of asteroid impactors. The model accounts for planetary migration/instability early in the solar system history and tracks asteroid orbits over 4.56 Gy. It is calibrated on the current population of the asteroid belt. The model provides the number of asteroid impacts on different worlds at any time throughout the solar system history. We combine the results with an impactor-crater scaling relationship to determine the crater distribution of Ceres and Vesta and compare these theoretical predictions with observations. We find that: (i) The Ceres and Vesta chronologies are similar, whereas they significantly differ from the lunar chronology. Therefore, using the lunar chronology for main belt asteroids, as often done in previous publications, is incorrect. (ii) The model results match the number and size distribution of large (diameter > 90 km) craters observed on Vesta, but overestimate the number of large craters on Ceres. This implies that large crater erasure is required for Ceres. (iii) In a model where planetary migration/instability happens early, the probability to form the Rheasilvia basin on Vesta during the last 1 Gy is 10%, a factor of ~ 1.5 higher than for the late instability case and ~ 2.5 times higher than found in previous studies. Thus, while the formation of the Rheasilvia at ~ 1 Gy ago (Ga) would be somewhat unusual, it cannot be ruled out at more than $\simeq 1.5\sigma$. In broader context, our work provides a self-consistent framework for modeling asteroid crater records.

Keywords: Main belt asteroids — Ceres — Solar system formation — Collision processes

1. INTRODUCTION

The crater chronology expresses the crater production rate (number of craters per unit time per surface area) as a function of time. It encapsulates our understanding of the observed crater record on surfaces of different bodies. If known, it can be used to estimate the surface age, identify the dominant populations of impactors, and infer interesting things about the dynamical and collisional evolution of the solar system. Unfortunately, it is quite difficult to determine an accurate crater chronology from data alone. This is because the ages of different craters are often unknown and must be inferred by indirect means. The only crater chronology that is directly derived from observational data is the lunar chronology (e.g. [Neukum et al. 2001](#); [Marchi et al. 2009](#); [Robbins 2014](#)). The Moon has a well preserved crater record and the soil samples returned by lunar missions can be used to infer accurate absolute ages of at least some lunar craters and basins. This provides time anchors from which the lunar chronology can be reconstructed.

For most other solar system bodies, for which the crater record is not well preserved and/or the absolute crater ages are unknown, the crater chronology must be inferred by different means (e.g. [Marchi et al. 2010](#); [Marchi et al. 2012a](#); [O’Brien et al. 2014](#); [Marchi et al. 2016](#)). For example, some researchers have re-scaled the lunar chronology to other bodies ([Marchi et al. 2009](#); [Schmedemann et al. 2014](#)), including the main belt asteroids, even if this method may be difficult to justify ([O’Brien et al. 2014](#)). Another approach, which we pursue here, is to model the evolution of impactors and their impacts on target bodies, and use the scaling laws ([Holsapple & Housen 2007](#); [Miljković et al. 2016](#); [Johnson et al. 2016](#)) to determine the expected crater distributions. The results are then compared to observations.

Before 2011 our knowledge of the asteroid crater records was based on spacecraft images of ~ 10 of these bodies, all of them smaller than 100 km in diameter. The arrival of the *Dawn* spacecraft to Vesta in 2011 and Ceres in 2015 opened a new window into studies of impact cratering in the asteroid belt. A large basin on Vesta’s surface have been suggested to explain the Vesta’s collisional family ([Binzel & Xu 1993](#)). It was later imaged by the Hubble Space Telescope ([Thomas et al. 1997](#)) and *Dawn*, and found to be $\simeq 500$ km in diameter (named Rheasilvia). *Dawn* has also discovered another basin on Vesta, now called Veneneia, roughly 400 km in diameter ([Marchi et al. 2012b](#)). In contrast, Ceres’s surface does not show any obvious basins and the largest craters, Kerwan and Yalode, have diameters of only 280 km and 260 km, respectively ([Marchi et al. 2016](#)). This is puzzling because Ceres has a collisional cross-section that is ~ 4 times larger than Vesta. For two of Vesta’s basins, there should thus be ~ 8 basins on Ceres, but there is none.

Previous attempts to derive a crater chronology for Vesta have been carried out by [Schmedemann et al. \(2014\)](#) and [O’Brien et al. \(2014\)](#). The former work used the lunar chronology and rescaled it, by simply multiplying the crater production rate by a fixed factor, to Vesta. They estimated the Rheasilvia and Veneneia age to be ~ 3.5 Gy. This is a significantly older age of Rheasilvia than the one (~ 1 Gy) suggested in [Marchi et al. \(2012b\)](#). At least part of this difference is due to different crater counting strategies adopted by different research teams. The young age of Rheasilvia would be more in line with the age of the Vesta family, thought to form in aftermath of the Rheasilvia impact, which was estimated from arguments based on the collisional grinding of family members ([Marzari et al. 1996](#)). Dynamical modeling of the Vesta family does not constrain the family age well and admits ages ≥ 1 Gy ([Carruba et al. 2005](#); [Nesvorný et al. 2008](#)), which are compatible with either age estimate mentioned above.

O’Brien et al. (2014) developed a new chronology for Vesta based on a synthesis of previous results. Their chronology accounts for the long-term dynamical depletion of the asteroid belt (Minton & Malhotra 2010), effects of planetary migration/instability and scattering by planetary embryos that may have resided in the belt during the earliest stages (Petit et al. 2001; O’Brien et al. 2007; Morbidelli et al. 2010). Their chronology implies the Rheasilvia age to be ~ 1 Gy and creates some tension with the low probability of forming Rheasilvia this late ($\sim 4\%$ according to O’Brien et al. 2014). They also pointed out a significant difference between the lunar and Vesta chronologies, suggesting that the flux of impactors on Vesta was *not* orders of magnitude higher during the lunar Late Heavy Bombardment (LHB).

A similar analysis was published for Ceres in Hiesinger et al. (2016) and Marchi et al. (2016). The former work applied both the lunar and O’Brien chronologies to Ceres and determined a relatively young age of the Kerwan crater (550-720 My). The absence of (obvious) large basins on Ceres is puzzling. Marchi et al. (2016) proposed that some large depressions observed on the Ceres’s surface, referred to as *planitia*, could be strongly relaxed basins. They identified at least two of these topological features, Vendimia planitia with a ~ 830 km diameter and another planitia with a ~ 570 km diameter. Various geological mechanisms related to crustal relaxation, including potentially recent geologic activity, could be responsible for nearly complete basin erasure.

Here we determine the crater chronologies of Ceres, Vesta and the Moon using a dynamical model of the asteroid belt from Nesvorný et al. (2017). See that work for a complete description of the model. In brief, the model accounts for the early dynamical evolution of the belt due to migration/instability of the outer planets and tracks asteroid orbits to the present epoch. The main asteroid belt, well characterized by modern surveys, is then used to calibrate the number and orbits of asteroids at any given time throughout the solar system history. The model does not account for other effects, such as scattering by planetary embryos, or other impactor populations, such as comets, leftovers of the terrestrial planet accretion, etc. In Sect. 2, we describe the model in more detail and explain the method that we used to determine the crater chronology and size distribution. The results for Vesta and Ceres are discussed in Sect. 3. Sect. 4 summarizes our main conclusions.

2. MODEL

2.1. Dynamical model

We use the dynamical model of Nesvorný et al. (2017) to determine the crater chronologies of Ceres and Vesta. In that work, we performed a numerical simulation –labeled as CASE1B– of 50,000 test asteroids over the age of the solar system. The simulation starts at the time of the solar nebula dispersal (it does not account for gas drag). The adopted physical model takes into account gravitational perturbations of all planets from Venus to Neptune (Mercury is included for $t \leq t_{\text{inst}}$, where t_{inst} is the time of dynamical instability; see below). During the early stages, the giant planets are assumed to evolve by planetesimal-driven migration and dynamical instability (the so-called jumping-Jupiter model; Morbidelli et al. 2009; Bottke et al. 2012; Nesvorný & Morbidelli 2012). See Nesvorný (2018) for a review. The simulations span 4.56 Gy and the time of the instability time t_{inst} is considered to be a free parameter. The Yarkovsky effect and collisional evolution of the main belt is not modeled in Nesvorný et al. (2017). This limits the reliability of the model to large asteroids for which these effects are not overly significant (Nesvorný & Roig 2018). Comets and other

impactor populations are not considered. This is equivalent to assuming that Ceres and Vesta crater records are dominated by asteroid impactors.

The dynamical model of Nesvorný et al. (2017) employed a flexible scheme to test any initial orbital distribution of asteroids. By propagating this distribution to the present time and comparing it with the observed distribution of main belt asteroids, we were able to reject models with too little or too much initial excitation (also see Roig & Nesvorný 2015). From the models that passed this test we select the one that has the Gaussian distributions in e and i with $\sigma_e = 0.1$ and $\sigma_i = 10^\circ$, and a power-law radial surface density $\Sigma(a) = 1/a$. We also tested other initial distributions, such as the one produced by the Grand Tack model (Walsh et al. 2011), and will briefly comment on them in Sect. 3. The Grand Tack distribution is wider in eccentricity (approximately Gaussian with $\sigma_e \simeq 0.2$ and Rayleigh in i with $\sigma_i \simeq 10^\circ$; see Roig & Nesvorný 2015 for explicit definitions of these distributions).

The impact probability and velocity of a test asteroid on a target world is computed by the Öpik algorithm (Bottke et al. 1994). This allows us to account for impacts on bodies that were not explicitly included in the simulation, such as Ceres, Vesta or the Moon. Ceres and Vesta are placed on their current orbits since time zero (corresponding to the dispersal of the protosolar nebula). This is only an approximation because in reality both these asteroids must have experienced orbital changes during the planetary migration/instability. Establishing how these changes may have affected their crater records is left for future work. See Nesvorný et al. (2017) for the method used for the Moon. The impact probabilities are initially normalized to 1 test particle surviving at the end of the simulation. In other words, the impact probabilities directly provided by a given simulation are divided by the total number of test particles that survived at the end of that simulation. This normalization is necessary, because the final state of the simulation resembles well the present asteroid belt only in terms of orbital distribution, but not in absolute numbers. The actual impact flux is obtained by multiplying these normalized impact probabilities by the number of asteroids larger than a given size in the present asteroid belt (see Eq. (1) below).

2.2. Crater chronology

The usual approach to modeling crater records of planetary and minor bodies consists of two steps. In the first step, scientists define the chronology function, $f(t)$, which gives the crater production rate as a function of time t . In the second step, the model production function (MPF), $n(D_{\text{crat}})$, is synthesized from available constraints to compute the crater production rate as a function of crater diameter, D_{crat} . The number of craters is then computed as $n(t, D_{\text{crat}}) = f(t) n(D_{\text{crat}}) dt dD_{\text{crat}}$. Integrating this relationship over t and/or D_{crat} leads to cumulative distributions (e.g., the number of craters larger than diameter D_{crat} produced since time t). This approach implicitly assumes that MPF is unchanging with time which may not be accurate if size-dependent processes such as the Yarkovsky effect (Vokrouhlický et al. 2015) influence the impactor population. We do not investigate such processes here.

Here we use a notation where t measures time from time zero, corresponding to the dispersal of the protosolar gas nebula, to the present epoch ($t = 0$ to 4.56 Gy) and T measures time backward from the present epoch to time zero; thus $T = 4.56 \text{ Gy} - t$. We first define the chronology function and MPF in terms of the *impactor* flux and diameters (the conversion method from impactor properties to craters is described in Sect. 2.3). The cumulative number of impacts, $n(T, D_{\text{ast}})$, of asteroids

larger than the diameter D_{ast} in the last T , is

$$n(T, D_{\text{ast}}) = F(T) \mathcal{N}(> D_{\text{ast}}) \quad (1)$$

where $\mathcal{N}(> D_{\text{ast}})$ is the current number of main belt asteroid larger than D_{ast} and $F(T)$ is the cumulative chronology function obtained from the dynamical model (here normalized to one asteroid larger than D_{ast} at $T = 0$). Eq. (1) represents a forward-modeling approach that is independent of any crater data; instead, it relies on the accuracy of numerical simulations to reproduce the main belt evolution and our understanding of the main belt size distribution (see Sect. 2.3).

Having the chronology function, the intrinsic impact probability (actually, the expected value of a Poisson distribution) on the target world, P_i , can be obtained as:

$$P_i(T) = \frac{4\pi}{S} \frac{dF(T)}{dT} \quad (2)$$

where S is the surface area of the target and the factor 4π accounts for the difference between the surface area and the cross section. With this definition of P_i , the total number of impacts is given as $P_i R^2 n \Delta t$, where R is the target radius, n is the number of impactors and Δt is the time interval. The model gives $P_i(0) \simeq 4.1 \times 10^{-18} \text{ km}^{-2} \text{ y}^{-1}$ for both Ceres and Vesta. This is somewhat higher than the mean value $P_i = 2.85 \times 10^{-18} \text{ km}^{-2} \text{ y}^{-1}$ usually considered for the whole asteroid belt (Farinella & Davis 1992). For Ceres, Marchi et al. (2016) found $P_i = 3.55 \times 10^{-18} \text{ km}^{-2} \text{ y}^{-1}$, which is more consistent with our $P_i(0)$. The small difference can be related to the fact that our model distribution of main belt asteroids is more concentrated towards smaller semimajor axes, because the model does not account the presence of large collisional families at $a \gtrsim 3$ au (mainly the Themis, Hygiea and Eos families). The mean impact velocities computed from our model are in the range of 4.6 to 7 km s^{-1} for the whole simulated time interval. They show a slightly decreasing trend with t during the earliest stages as asteroid impactors on high- e orbits are removed. The mean velocity at $T = 0$ is in good agreement with the current value (Bottke et al. 1994).

2.3. Size distribution

A general procedure to analytically estimate the MPF has been outlined in Marchi et al. (2009). A limitation of this procedure arises from uncertainties in modeling the processes of crater erasure such as, in particular, the obliteration of older and smaller craters by newer and larger ones. The crater erasure can be included in the MPF through a weight function, as explained in O'Brien et al. (2006) and Marchi et al. (2009). Here we instead develop a Monte Carlo approach to forward model the crater size distribution (also see Marchi et al. 2016).

To simulate the formation of craters we combine the observed size distribution of the main belt asteroids with the chronology functions obtained from our dynamical model. The size distribution is constructed from the WISE/NEOWISE observations (Masiero et al. 2011; Mainzer et al. 2019)¹, which is practically complete down to $D_{\text{ast}} \simeq 9\text{-}10$ km. For diameters slightly smaller than that, we adopt an extrapolation $\mathcal{N} = 10^\alpha D_{\text{ast}}^{-\gamma}$, where $\alpha = 6.5$, $\gamma = -2.6$ for the distribution of the whole main belt, and $\alpha = 6.23$, $\gamma = -2.54$ for the main belt background, i.e. subtracting the members of known asteroid families. These extrapolations were obtained by fitting the size distribution of asteroids slightly larger than 10 km by a power law and extending the power law below 10 km.

¹ Available at the NASA PDS Small Bodies Node, <https://sbn.psi.edu/pds/resource/neowisediam.html>

Our model consists of the following steps:

1. We define the minimum impactor diameter, $D_{\text{ast},0}$, that needs to be accounted for to match the smallest craters that we want to model.
2. We use Eq. (1) to determine the average number of impacts $\bar{n}_{\text{imp}} = n(T, D_{\text{ast},0})$ at $T = 0$ Ga.
3. We draw the actual number of impacts n_{imp} over the desired time span from a Poisson distribution with mean \bar{n}_{imp} .
4. We generate n_{imp} craters from main belt impactors larger than $D_{\text{ast},0}$ using the following procedure:
 - (a) From the main belt size distribution, we draw the size D_{ast} of the impactor (in m).
 - (b) From the chronology function, we draw the time T that will represent the crater age.
 - (c) We obtain the velocity v of the impact (in m s^{-1}) at the time T . Note that this is more accurate than just drawing a value from the overall impact velocity distribution, because velocities are slightly higher at earlier times.
 - (d) We set the impact angle $\theta = 45^\circ$ (Shoemaker 1962).
 - (e) We compute the crater diameter D_{crat} (in m) using the scaling law from Johnson et al. (2016) for non-porous targets:

$$D_{\text{crat}} = 1.52 D_{\text{ast}}^{0.88} v^{0.5} (\sin \theta)^{0.38} \left(\frac{\delta}{\rho}\right)^{0.38} g^{-0.25} D_{\text{sc}}^{-0.13}. \quad (3)$$

Here, δ is the impactor’s density, ρ is the target’s density, g is the target’s surface gravity (in m s^{-2}), and D_{sc} is the simple-to-complex transition diameter (i.e., the diameter for which the crater starts to develop complex structures, such as multiple ridges, concentric rings, etc.). The values of these parameters adopted here for Ceres and Vesta are given in Table 1.

5. We assign to each crater the initial weight $W = 1$.
6. To account for crater erasure, we consider, one by one, the model-generated craters with size D_{crat} and age T . We then select all craters with sizes $< D_{\text{crat}}$ and ages $> T$, and subtract from their weights an amount $\pi D_{\text{crat}}^2 / (4S)$, which is the ratio of the crater surface area to the body surface area. When W becomes 0, the corresponding crater is assumed to be totally obliterated. This recipe is designed to model the crater overlap only, i.e. a “cookie cutting” approach.
7. The final size distribution of craters is obtained by adding all weights of craters with diameter D_{crat} together.
8. The steps (3) to (7) are repeated 1000 times to build up statistics. We compute the mean and the 1σ uncertainty of crater size distributions and compare them to observations.
9. Optionally, we can include formation of a large basin at a specific time. This is done, for example, to test the erasure of older and smaller craters by the Rheasilvia basin formation.

The crater erasure algorithm in step (4) is a simple method that only accounts for crater overlap. It does not take into account, for example, that the material ejected from large craters may degrade/bury small craters at considerable distance from the impact site. It is therefore expected that our method could underestimate the erasure of small craters. Here, however, we restrict our analysis to $D_{\text{crat}} > 50$ km craters for which this effect may not be important.

2.4. Caveats

As a by-product of the procedure outlined above we obtain a set of D_{crat} vs. D_{ast} values indicating that the scaling law in Eq. (3) approximately follows a linear dependence $D_{\text{crat}} \simeq f_{\text{sl}} \times D_{\text{ast}}$, where f_{sl} is a constant factor, at least in the size range considered here. The typical values of f_{sl} are in the range ~ 11 -13 for Ceres and ~ 8 -10 for Vesta. Therefore, if we want to fit the size distribution of craters with $D_{\text{crat}} > 60$ km, we have to set $D_{\text{ast},0} \sim 6$ km in the case of Vesta and $D_{\text{ast},0} \sim 4$ km in the case of Ceres. This creates a problem because the dynamical model used here is strictly reliable only for $D_{\text{ast}} \gtrsim 10$ km (because it does not account for the size-dependent processes such as the Yarkovsky effect or collisional fragmentation).

The Yarkovsky drift of a $D_{\text{ast}} = 4$ km asteroid is expected to be ~ 0.04 au Gy $^{-1}$. The drift may be directed inward or outward, depending on asteroid's spin axis orientation. The intrinsic collision probability of the target is not expected to be significantly affected by this, because the inward and outward drifts would average out (assuming a random orientation of spin axes). The main effect of the Yarkovsky drift should consist in larger depletion of small main belt asteroids relative to our size-independent model where asteroid orbits are expected to be more stable. This could potentially mean that the chronology function would have a somewhat steeper dependence with time for $D_{\text{ast}} < 10$ km than for $D_{\text{ast}} > 10$ km impactors. The investigation of this effect is left for future work.

The effects of collisional grinding are difficult to estimate. The collisional grinding removes mass over time and thus reduces the population of small asteroids. This happens on the top of the dynamical depletion. The general expectation is that the belt should evolve faster initially when it is still massive (Bottke et al. 2005). Recall that we anchor the results of our dynamical model to the *current* population of small asteroids. Thus, running the clock back in time, our model must underestimate the actual number of impacts (because it does not account for impactors that were collisionally eliminated).

The formation of asteroid families over the age of the solar system contributes to enhance the two effects discussed above, but it has also another consequence. There are several large collisional families in the outer asteroid belt (Themis, Hygiea and Eos families) and these families have many $D_{\text{ast}} \sim 10$ km members (Nesvorný et al. 2015; Nesvorný 2015). Including these bodies in our calibration effectively means that we assume that all these families existed for the whole duration of our simulation (i.e., formed 4.56 Ga), which is clearly not the case because, for example, the Eos family formed only ~ 1.3 Ga (Vokrouhlický et al. 2006). To test how this approximation affects our results, we can remove asteroid families from the main belt and calibrate our chronology on the current main belt background. These tests show a variation in the number of impacts by a factor of ~ 2 . The uncertainty of our results, described below, cannot be better than that.

Finally, another possible source of uncertainty is the contribution to the collisional rates in the main belt of the population of Hungaria asteroids, which may have constituted a significant early population depending on the eccentricity history of Mars (Čuk & Nesvorný 2018). Model CASE1B from Nesvorný et al. (2017) does account for a primordial population of asteroids in the range

$1.6 < a < 2.1$ au, the so called E-belt (Bottke et al. 2012). Therefore, the derived production functions and chronologies used here include the effects of this population. However, model CASE1B did not reproduce well the currently observed population of Hungarias, because the E-belt became more depleted than it should, especially at later times (Roig & Nesvorný 2015). In any case, the uncertainty introduced by this effect is small and would be within the factor of 2 discussed above.

3. RESULTS

3.1. Comparison of lunar and asteroid chronologies

The chronology functions obtained in our model for Vesta, Ceres and the Moon are compared in Fig. 1. The lunar chronology shows a vast number of impacts during the early epochs when the impactor flux is at least ~ 2 orders of magnitude higher than at the present time (Nesvorný et al. 2017). This happens because many main belt asteroids become destabilized during the planetary migration/instability and evolve into the terrestrial planet region, which leads to a strong asteroid bombardment of the Moon and terrestrial planets. In contrast, the impact flux on Vesta and Ceres is more unchanging with time. This happens because Vesta and Ceres orbit within the main belt and are continuously impacted by asteroids. For them, the early bombardment is not as dramatic as for the Moon. This means that the lunar chronology does not apply to Vesta or Ceres. These considerations also imply that Vesta’s and Ceres’s craters should be on average younger than the lunar craters.

O’Brien et al. (2014) reached similar conclusions. To illustrate this, we show the Vesta chronology from O’Brien et al. (2014) in Fig. 1b. We used Eqs. (16) and (18) in their paper and scaled their MPF (their figure 1) assuming a linear scaling law with $8 \leq f_{sl} \leq 20$. Note that $f_{sl} \sim 9$ reproduce well the scaling law of Johnson et al. (2016) for Vesta. We would therefore expect that our results for Vesta should plot near the upper limit of their chronology function range, and this is indeed the case. In O’Brien et al. (2014), the Vesta’s chronology was pieced together from several publications and was compared with the lunar chronology of Neukum et al. (2001) (which was obtained by yet another method). The advantage of our approach is that all chronologies are derived from a single, self-consistent physical model.

3.2. Impact flux for early and late instabilities

The time of planetary migration/instability is a crucial parameter for the Moon as it substantially changes the lunar impact flux during early stages and the overall number of impacts (Fig. 1a). Vesta’s and Ceres’s impact records are much less sensitive to this parameter. Indeed, Fig. 1a shows that the records are nearly identical for $T_{inst} = 4.5$ Ga and $T_{inst} = 3.9$ Ga. We therefore do not expect to find many clues about the LHB or the early evolution of the giant planets by analyzing the crater record of these asteroids. Given that other available constraints indicate that the instability happened early (Nesvorný et al. 2018), we give preference to the early instability case in the rest of the paper. We find no appreciable difference for the Gaussian and Grand Tack initial distributions. The Gaussian initial distribution, as described in Sect. 2.1, is used in the following analysis.

The early instability model suggests that the Moon should have registered ~ 27 impacts from $D_{ast} > 9$ km asteroids over the age of the solar system (see also Nesvorný et al. 2017), while Ceres and Vesta registered ~ 51 and ~ 16 such impacts, respectively (Fig. 1b). According to O’Brien et al. (2014), Vesta would have registered between 10 and 75 impacts of $D_{ast} > 9$ km asteroids, but $\sim 70\%$ of these impacts would have occurred during the first 50 My of evolution. In general, O’Brien

et al.’s chronology produces ~ 1.5 times fewer impacts per Gy during the last ~ 4 Gy than our chronology (assuming $f_{sl} \sim 9$). This discrepancy is, at least in part, related to the fact that O’Brien et al.’s chronology shows a drop at the very beginning, reflecting their attempt to account for strong depletion of the main asteroid belt by processes not modeled here (e.g., planetary embryos, Grand Tack).²

Marchi et al. (2016) derived a chronology function for Ceres that has a very similar shape to O’Brien et al.’s chronology for Vesta. It also shows a drop during the first 50 My of evolution due to a presumably strong primordial depletion of the main belt. Using this chronology, they predicted 180 and 90 impacts from impactors with $D_{ast} > 10$ km and $D_{ast} > 13$ km, respectively. According to their scaling laws, these impactors produce craters with $D_{crat} \sim 100$ km. About 70% of these impacts happen during the first 400 My of evolution (i.e. before the dynamical instability that they place at 4.1 Ga). Compared to that, our model implies ~ 4 times fewer impacts and we do not find any significant difference between the number of impacts for the early and late instability cases. The number of craters of various sizes expected from our model is reported in Table 2. For Vesta, these numbers are in a good agreement with observations, especially if we account for modest crater erasure (see Sect. 2.3). For Ceres, strong crater erasure by viscous relaxation may be required (Sect. 3.4).

3.3. Vesta’s craters

Figure 2 compares our model size distributions of Vesta’s craters to observations. To introduce this comparison, recall that we have blindly taken a dynamical model of the asteroid belt evolution (i.e., without any a priori knowledge of what implications the model will have for the Vesta’s crater record) and used a standard scaling law to produce the crater record. There is not much freedom in this procedure. If the dynamical model were not accurate, for example, we could have obtained orders of magnitude more or less craters than what the *Dawn* mission found. But this is not the case. In fact, there is a very good general agreement between the model results and observations. This also shows that the caveats discussed in Sect. 2.4 do not (strongly) influence the results.

In more detail, in a model where no crater erasure is taken into account (left panel of Fig. 2), the agreement is excellent for craters with $D_{crat} > 100$ km. There is a small difference for $D_{crat} \lesssim 100$ km, where the model distribution steeply raises and slightly overestimates the number of craters. A similar problem was identified in O’Brien et al. (2014). We tested whether this issue may be a result of crater erasure. Indeed, when crater erasure is included in the model (the middle panel of Fig. 2), the size distribution shifts down and becomes slightly shallower. It now better fits the data in the whole range modeled here. The results do not change much when we include the presumed Rheasilvia basin formation at ~ 1 Gy ago (right panel of Fig. 2).³

In summary, our model works really well to reproduce the Vesta’s crater record and a modest crater erasure may be needed to better fit the number of $D_{crat} \lesssim 100$ km craters.

3.4. Ceres’s craters

² The strong depletion of the asteroid belt was thought to be needed, because the formation models based on the minimum mass solar nebula suggested that the primordial mass of the main belt was 100-1000 times larger than the present one (Weidenschilling 1977). Also, the classical model of asteroid accretion by collisional coagulation required a large initial mass to produce 100-km class objects. The formation paradigm has shifted, however, with more recent models favoring a low initial mass (Morbidelli et al. 2015).

³ If the dynamical model is calibrated on the main belt background (i.e., asteroid families removed; Sect. 2.4), we obtain ~ 2 times fewer craters. This does not make much of a difference on the logarithmic scale in Fig. 2, but the overall fit without crater erasure becomes slightly better.

Figure 3 shows a similar comparison for Ceres. In this case, the model without crater erasure predicts nearly an order of magnitude more craters on Ceres’s surface than the number of actual craters. A similar problem was noted in [Marchi et al. \(2016\)](#). The situation improves when the crater erasure is included in the model (middle panel of Fig. 3), but the problem is not entirely resolved. We could have tried to erase craters more aggressively, for example, by assuming that small craters are degraded by distal ejecta from large craters ([Minton et al. 2019b](#)). But this would create problems for Vesta where the model with our conservative erasure method (craters must overlap to be erased) worked quite well. Actually, [Minton et al. \(2019b\)](#) showed that crater degradation by energetic deposition of ejecta (e.g. secondary cratering/ballistic sedimentation) on the Moon works differently for the larger craters comparable to the crater sizes considered here ([Minton et al. 2019a](#)), so that mechanism would probably not be applicable in the cases of Ceres and Vesta.

Following [Marchi et al. \(2016\)](#), we therefore investigate the effects of viscous relaxation (which are specific to ice-rich Ceres). To empirically incorporate the effects of viscous relaxation in our model, we assume that the model weight of each crater diminishes according to the following prescription:

$$W = \exp(-T/\tau) \quad (4)$$

where e-folding timescale is a function of crater diameter,

$$\tau = C/D_{\text{crat}} \quad (5)$$

as supported by classical models of relaxation on icy surfaces (e.g. [Johnson & McGetchin 1973](#); [Bland et al. 2012](#); [Bland 2013](#)). Here, $C = 4\pi\eta/\rho g$ is a constant depending on the viscosity η of the surface layer.

The right panel of Fig. 3 shows the model results for Ceres considering crater erasure together with viscous relaxation. In this case, we are able to fit the observed crater record assuming a value of $C \simeq 200 \text{ km Gy}$, which would imply a surface viscosity of $\sim 3 \times 10^{23} \text{ Pa s}$. This is about three orders of magnitude larger than the viscosity of pure ice at 180 K (the approximate temperature of Ceres surface), meaning that the particulate content volume in the icy surface layer needs to be significant. In fact, viscous relaxation of a purely icy surface is expected to be an aggressive process, with a typical e-folding timescale of only 1 My for the erasure of topographic wavelengths as short as 100 km. Our result is in line with more rigorous studies of the Ceres internal structure ([Fu et al. 2017](#)), which infer a mechanically strong crust, with maximum effective viscosity $\sim 10^{25} \text{ Pa s}$.

This gives some support to the viscous relaxation prescription discussed above. We caution, however, that the results are likely not unique and different combinations of crater erasure and viscous relaxation prescriptions (e.g., more aggressive crater erasure and longer viscous relaxation timescale) could produce similarly good fits.

In summary, we find that both erasure processes should be important for Ceres and $D_{\text{crat}} \sim 100 \text{ km}$ Ceres’s craters should viscously relax on an e-folding timescale of $\sim 1\text{-}2 \text{ Gy}$. This represents an interesting constrain on geophysical models of viscous relaxation and Ceres’s composition.

3.5. Basins formation

Here, we discuss the probability of forming large craters or basins ($D_{\text{crat}} > 400 \text{ km}$) on Vesta and Ceres at different times in the past. One possible approach to this problem consists in computing the so-called isochrones for each body, i.e. the crater production function at different times T . For

a given diameter D_{crat} , each isochrone gives the expected number of craters $\mu(> D_{\text{crat}}, < T)$, and the probability of forming exactly N (and only N) craters $> D_{\text{crat}}$ in a time $< T$ is obtained from a Poisson distribution:

$$p_{\mu}(N) = \frac{\mu^N e^{-\mu}}{N!} \quad (6)$$

Figure 4 shows the isochrones for Ceres and Vesta, as determined from our model, without considering any crater erasure. If we take the case of a 500 km basin on Vesta, we find that the expected value for the $T = 1$ Ga isochrone is $\mu = 0.10$, and from Eq. (6) the probability of forming one basin is 9%, while the probability of forming two basins is much smaller, 0.5%. However, if we consider the $T = 4.56$ Ga isochrone, the probability of forming two basins increases to 4.6%. We recall that the probability of forming at least one 500 km basin in the last 1 Gy can be obtained as $1 - p_{\mu}(0)$, which in this case would give a value of 9.5%. Table 3 summarizes the results for $D_{\text{crat}} > 400$ km.

Another possible approach consists in using our model to directly determine the probability of producing at least N craters larger than a given size over a certain time span. This approach differs from the previous one in that it does not rely on the Poisson statistics, but on the output of the Monte Carlo simulations. Figure 5 shows the probability of creating at least one crater (panel a) and at least two craters (panel b) larger than a cutoff diameter on Vesta. Again, no crater erasure is considered here. We find that the probability of creating the Rheasilvia basin with $D_{\text{crat}} \simeq 500$ km (the cyan line in panel a) in the last 1 Gy (or 2 Gy) is 10% (or 18%). This is about 2.5 times more likely than the probability reported in O’Brien et al. (2014). This happens because our chronology function leaves more space for a relatively late formation of craters/basins. O’Brien et al. (2014), instead, adopted a strong primordial depletion and had more basins forming early on (e.g. O’Brien et al. 2007). If we consider $D_{\text{crat}} > 400$ km (blue line in panel a), the probabilities of forming at least one crater become 14% in the last 1 Gy, and 25% in the last 2 Gy. These values are slightly larger than those reported in Table 3, because the Poisson statistics constrains the formation of exactly N craters.

The probability of forming both the Rheasilvia and Veneneia basins (the blue line in Fig. 5b corresponding to $D_{\text{crat}} = 400$ km) is 15% over the age of the solar system, and 6% in the last 3 Ga. Again, these values are slightly larger than those reported in Table 3. Table 4 reports different probabilities assuming that the age of Rheasilvia is ≤ 1 Gy (note that we do not claim that this is an accurate age of the Rheasilvia basin; we merely test this assumption) and Veneneia is > 1 Gy, for the models with early and late instabilities. The probabilities are slightly higher in the early instability model simply because, in this model, the rate of impacts is slightly higher in the past 1 Gy. Thus, a young age for Rheasilvia could potentially be more consistent with an early instability model. In any case, our chronology still implies that most Vesta’s craters/basins should have preferentially formed early in the solar system history.

Figure 6 shows the results for Ceres. In this case, the probability of *not* creating any basin with $D_{\text{crat}} > 400$ km over the age of the solar system is only 1% (the red line in Fig. 6). Combining this result with the one for Vesta (see above) we estimate that the joint probability of creating two $D_{\text{crat}} > 400$ km basins on Vesta younger than 3 Gy and no $D_{\text{crat}} > 400$ km basin on Ceres is only $< 0.1\%$. Figure 7 shows, at the top, the one exceptional case we found over 1000 realizations that fulfills the above condition. For comparison, an example of the typical outcome of our Monte Carlo model is shown at the bottom. This result emphasizes the need for efficient removal of Ceres’s basins by viscous relaxation (or some other process).

4. CONCLUSIONS

Our findings can be summarized as follows:

- The crater chronologies of Ceres and Vesta are very different from that of the Moon. This is a consequence of the fact that both Vesta and Ceres spent their whole lifetimes in the asteroid belt and are impacted all the time, whereas the Moon experienced a more intense bombardment during the first ~ 1 Gy. This means that using the lunar chronology for Ceres and Vesta is incorrect. The scaled lunar chronology would imply that Vesta's basins must have formed very early in the solar system history, which may not necessarily be the case.
- Our crater chronologies of Ceres and Vesta are similar to those obtained in some previous studies (O'Brien et al. 2014; Marchi et al. 2016). In our chronology, however, the crater ages are not as concentrated toward the early times as in these works, allowing more impacts in the past 3 Gy.
- The model crater record of Vesta matches observations (e.g., 10 known craters with $D_{\text{crat}} > 90$ km). The model with crater erasure overpredicts, by a factor of ~ 3 , the number of $D_{\text{crat}} > 90$ km craters observed on the Ceres's surface. An additional erasure process such as, for example, the size-dependent viscous relaxation of craters (with ~ 2 Gy timescale for $D_{\text{crat}} = 100$ km craters), may be responsible for this discrepancy.
- We estimate that the probability of creating the Rheasilvia and Veneneia basins ($D_{\text{crat}} > 400$ km) on Vesta during the last 3 Gy is $\simeq 6\%$, somewhat larger than found in the previous studies. A recent formation of the Rheasilvia basin can be more easily accepted in a dynamical model with the early instability, where the impact probabilities in the last 1 Gy are higher.
- The probability of producing two large basins ($D_{\text{crat}} > 400$ km) on Vesta and simultaneously not producing any basin on Ceres is interestingly small ($< 0.1\%$). The relative paucity of large craters/basins on Ceres may be explained in a model with crater erasure and viscous relaxation.

ACKNOWLEDGMENTS

The authors wish to thank David Minton for helpful comments and suggestions during the revision of this paper. FR's work was supported by the Brazilian National Council of Research (CNPq). DN's work was supported by the NASA SSERVI and SSW programs. The simulations were performed on the SDumont computer cluster of the Brazilian System of High Performance Processing (SINAPAD).

REFERENCES

- Binzel, R. P., & Xu, S. 1993, *Science*, 260, 186, doi: [10.1126/science.260.5105.186](https://doi.org/10.1126/science.260.5105.186)
- Bland, M. T. 2013, *Icarus*, 226, 510, doi: [10.1016/j.icarus.2013.05.037](https://doi.org/10.1016/j.icarus.2013.05.037)
- Bland, M. T., Singer, K. N., McKinnon, W. B., & Schenk, P. M. 2012, *Geophys. Res. Lett.*, 39, L17204, doi: [10.1029/2012GL052736](https://doi.org/10.1029/2012GL052736)
- Bottke, W. F., Durda, D. D., Nesvorný, D., et al. 2005, *Icarus*, 175, 111, doi: [10.1016/j.icarus.2004.10.026](https://doi.org/10.1016/j.icarus.2004.10.026)
- Bottke, W. F., Nolan, M. C., Greenberg, R., & Kolvoord, R. A. 1994, *Icarus*, 107, 255, doi: [10.1006/icar.1994.1021](https://doi.org/10.1006/icar.1994.1021)

- Bottke, W. F., Vokrouhlický, D., Minton, D., et al. 2012, *Nature*, 485, 78, doi: [10.1038/nature10967](https://doi.org/10.1038/nature10967)
- Carruba, V., Michtchenko, T. A., Roig, F., Ferraz-Mello, S., & Nesvorný, D. 2005, *A&A*, 441, 819, doi: [10.1051/0004-6361:20053355](https://doi.org/10.1051/0004-6361:20053355)
- Čuk, M., & Nesvorný, D. 2018, *Icarus*, 304, 9, doi: [10.1016/j.icarus.2017.04.015](https://doi.org/10.1016/j.icarus.2017.04.015)
- Farinella, P., & Davis, D. R. 1992, *Icarus*, 97, 111, doi: [10.1016/0019-1035\(92\)90060-K](https://doi.org/10.1016/0019-1035(92)90060-K)
- Fu, R. R., Ermakov, A. I., Marchi, S., et al. 2017, *Earth and Planetary Science Letters*, 476, 153, doi: [10.1016/j.epsl.2017.07.053](https://doi.org/10.1016/j.epsl.2017.07.053)
- Hiesinger, H., Marchi, S., Schmedemann, N., et al. 2016, *Science*, 353, aaf4758, doi: [10.1126/science.aaf4759](https://doi.org/10.1126/science.aaf4759)
- Holsapple, K. A., & Housen, K. R. 2007, *Icarus*, 187, 345, doi: [10.1016/j.icarus.2006.08.029](https://doi.org/10.1016/j.icarus.2006.08.029)
- Johnson, B. C., Collins, G. S., Minton, D. A., et al. 2016, *Icarus*, 271, 350, doi: [10.1016/j.icarus.2016.02.023](https://doi.org/10.1016/j.icarus.2016.02.023)
- Johnson, T. V., & McGetchin, T. R. 1973, *Icarus*, 18, 612, doi: [10.1016/0019-1035\(73\)90064-X](https://doi.org/10.1016/0019-1035(73)90064-X)
- Mainzer, A. K., Bauer, J. M., Cutri, R. M., et al. 2019, NASA Planetary Data System, urn:nasa:pds:neowise_diameters_albedos::2.0
- Marchi, S., Mottola, S., Cremonese, G., Massironi, M., & Martellato, E. 2009, *AJ*, 137, 4936, doi: [10.1088/0004-6256/137/6/4936](https://doi.org/10.1088/0004-6256/137/6/4936)
- Marchi, S., Barbieri, C., Küppers, M., et al. 2010, *Planet. Space Sci.*, 58, 1116, doi: [10.1016/j.pss.2010.03.017](https://doi.org/10.1016/j.pss.2010.03.017)
- Marchi, S., Massironi, M., Vincent, J.-B., et al. 2012a, *Planet. Space Sci.*, 66, 87, doi: [10.1016/j.pss.2011.10.010](https://doi.org/10.1016/j.pss.2011.10.010)
- Marchi, S., McSween, H. Y., O'Brien, D. P., et al. 2012b, *Science*, 336, 690, doi: [10.1126/science.1218757](https://doi.org/10.1126/science.1218757)
- Marchi, S., Ermakov, A. I., Raymond, C. A., et al. 2016, *Nature Communications*, 7, 12257, doi: [10.1038/ncomms12257](https://doi.org/10.1038/ncomms12257)
- Marzari, F., Cellino, A., Davis, D. R., et al. 1996, *A&A*, 316, 248
- Masiero, J. R., Mainzer, A. K., Gray, T., et al. 2011, *ApJ*, 741, 68, doi: [10.1088/0004-637X/741/2/68](https://doi.org/10.1088/0004-637X/741/2/68)
- Miljković, K., Collins, G. S., Wieczorek, M. A., et al. 2016, *Journal of Geophysical Research (Planets)*, 121, 1695, doi: [10.1002/2016JE005038](https://doi.org/10.1002/2016JE005038)
- Minton, D., Fassett, C., Hirabayashi, M., & Riedel, C. 2019a, in *EPSC-DPS Joint Meeting 2019*, Vol. 2019, EPSC–DPS2019–1065
- Minton, D. A., Fassett, C. I., Hirabayashi, M., Howl, B. A., & Richardson, J. E. 2019b, *Icarus*, 326, 63, doi: [10.1016/j.icarus.2019.02.021](https://doi.org/10.1016/j.icarus.2019.02.021)
- Minton, D. A., & Malhotra, R. 2010, *Icarus*, 207, 744, doi: [10.1016/j.icarus.2009.12.008](https://doi.org/10.1016/j.icarus.2009.12.008)
- Morbidelli, A., Brassier, R., Gomes, R., Levison, H. F., & Tsiganis, K. 2010, *AJ*, 140, 1391, doi: [10.1088/0004-6256/140/5/1391](https://doi.org/10.1088/0004-6256/140/5/1391)
- Morbidelli, A., Brassier, R., Tsiganis, K., Gomes, R., & Levison, H. F. 2009, *A&A*, 507, 1041, doi: [10.1051/0004-6361/200912876](https://doi.org/10.1051/0004-6361/200912876)
- Morbidelli, A., Walsh, K. J., O'Brien, D. P., Minton, D. A., & Bottke, W. F. 2015, in *Asteroids IV*, ed. P. Michel, F. E. DeMeo, & W. F. Bottke, 493–507, doi: [10.2458/azu_uapress_9780816532131-ch026](https://doi.org/10.2458/azu_uapress_9780816532131-ch026)
- Nesvorný, D. 2015, NASA Planetary Data System, EAR
- . 2018, *ARA&A*, 56, 137, doi: [10.1146/annurev-astro-081817-052028](https://doi.org/10.1146/annurev-astro-081817-052028)
- Nesvorný, D., Brož, M., & Carruba, V. 2015, in *Asteroids IV*, ed. P. Michel, F. E. DeMeo, & W. F. Bottke, 297–321, doi: [10.2458/azu_uapress_9780816532131-ch016](https://doi.org/10.2458/azu_uapress_9780816532131-ch016)
- Nesvorný, D., & Morbidelli, A. 2012, *AJ*, 144, 117, doi: [10.1088/0004-6256/144/4/117](https://doi.org/10.1088/0004-6256/144/4/117)
- Nesvorný, D., & Roig, F. 2018, *AJ*, 155, 42, doi: [10.3847/1538-3881/aa9a47](https://doi.org/10.3847/1538-3881/aa9a47)
- Nesvorný, D., Roig, F., & Bottke, W. F. 2017, *AJ*, 153, 103, doi: [10.3847/1538-3881/153/3/103](https://doi.org/10.3847/1538-3881/153/3/103)
- Nesvorný, D., Roig, F., Gladman, B., et al. 2008, *Icarus*, 193, 85, doi: [10.1016/j.icarus.2007.08.034](https://doi.org/10.1016/j.icarus.2007.08.034)
- Nesvorný, D., Vokrouhlický, D., Bottke, W. F., & Levison, H. F. 2018, *Nature Astronomy*, 2, 878, doi: [10.1038/s41550-018-0564-3](https://doi.org/10.1038/s41550-018-0564-3)
- Neukum, G., Ivanov, B. A., & Hartmann, W. K. 2001, *SSRv*, 96, 55
- O'Brien, D. P., Greenberg, R., & Richardson, J. E. 2006, *Icarus*, 183, 79, doi: [10.1016/j.icarus.2006.02.008](https://doi.org/10.1016/j.icarus.2006.02.008)
- O'Brien, D. P., Marchi, S., Morbidelli, A., et al. 2014, *Planet. Space Sci.*, 103, 131, doi: [10.1016/j.pss.2014.05.013](https://doi.org/10.1016/j.pss.2014.05.013)
- O'Brien, D. P., Morbidelli, A., & Bottke, W. F. 2007, *Icarus*, 191, 434, doi: [10.1016/j.icarus.2007.05.005](https://doi.org/10.1016/j.icarus.2007.05.005)

- Petit, J.-M., Morbidelli, A., & Chambers, J. 2001, *Icarus*, 153, 338, doi: [10.1006/icar.2001.6702](https://doi.org/10.1006/icar.2001.6702)
- Robbins, S. J. 2014, *Earth and Planetary Science Letters*, 403, 188, doi: [10.1016/j.epsl.2014.06.038](https://doi.org/10.1016/j.epsl.2014.06.038)
- Roig, F., & Nesvorný, D. 2015, *AJ*, 150, 186, doi: [10.1088/0004-6256/150/6/186](https://doi.org/10.1088/0004-6256/150/6/186)
- Scheeres, D. J., Britt, D., Carry, B., & Holsapple, K. A. 2015, in *Asteroids IV*, ed. P. Michel, F. E. DeMeo, & W. F. Bottke, 745–766, doi: [10.2458/azu_uapress_9780816532131-ch038](https://doi.org/10.2458/azu_uapress_9780816532131-ch038)
- Schmedemann, N., Kneissl, T., Ivanov, B. A., et al. 2014, *Planet. Space Sci.*, 103, 104, doi: [10.1016/j.pss.2014.04.004](https://doi.org/10.1016/j.pss.2014.04.004)
- Shoemaker, E. M. 1962, in *Physics and astronomy of the moon*, ed. Z. Kopal (New York: Academic Press), 283–359
- Thomas, P. C., Binzel, R. P., Gaffey, M. J., et al. 1997, *Icarus*, 128, 88, doi: [10.1006/icar.1997.5736](https://doi.org/10.1006/icar.1997.5736)
- Vokrouhlický, D., Bottke, W. F., Chesley, S. R., Scheeres, D. J., & Statler, T. S. 2015, in *Asteroids IV*, ed. P. Michel, F. E. DeMeo, & W. F. Bottke, 509–531, doi: [10.2458/azu_uapress_9780816532131-ch027](https://doi.org/10.2458/azu_uapress_9780816532131-ch027)
- Vokrouhlický, D., Brož, M., Morbidelli, A., et al. 2006, *Icarus*, 182, 92, doi: [10.1016/j.icarus.2005.12.011](https://doi.org/10.1016/j.icarus.2005.12.011)
- Walsh, K. J., Morbidelli, A., Raymond, S. N., O’Brien, D. P., & Mandell, A. M. 2011, *Nature*, 475, 206, doi: [10.1038/nature10201](https://doi.org/10.1038/nature10201)
- Weidenschilling, S. J. 1977, *Ap&SS*, 51, 153, doi: [10.1007/BF00642464](https://doi.org/10.1007/BF00642464)

Table 1. Values of different parameters adopted in the present study. See [Hiesinger et al. \(2016\)](#) for D_{sc} and [Scheeres et al. \(2015\)](#) for δ .

	Ceres	Vesta
Impactor density δ (g cm^{-3})	2.5	
Target density ρ (g cm^{-3})	2.08	3.42
Surface gravity g (ms^{-2})	0.273	0.253
Simple to complex transition D_{sc} (km)	10	60
Target surface S ($\times 10^5 \text{ km}^2$)	27.7	8.8
Minimum impactor diameter $D_{ast,0}$ (km)	4	6

Table 2. A comparison between the number of observed and model predicted craters for Vesta and Ceres. Each predicted number represents the expected value of a Poisson distribution over 4.56 Gy. The values for the early and late instability cases are reported. Here we do not account for any crater erasure process (Sect. 2.3)

Impactors (km)	Vesta			Ceres		
	Craters (km)	Observed [†]	Predicted Early / Late	Craters (km)	Observed [‡]	Predicted Early / Late
$D_{ast} > 8$	$D_{crat} > 70$	-	22 / 28	$D_{crat} > 90$	26	68 / 69
$D_{ast} > 9$	$D_{crat} > 80$	-	16 / 21	$D_{crat} > 100$	17	51 / 52
$D_{ast} > 10$	$D_{crat} > 90$	10	13 / 16	$D_{crat} > 110$	14	40 / 41
$D_{ast} > 11$	$D_{crat} > 100$	-	10 / 13	$D_{crat} > 120$	8	32 / 33
$D_{ast} > 12$	$D_{crat} > 110$	6	8 / 11	$D_{crat} > 130$	6	26 / 27

[†][Marchi et al. \(2012b\)](#)

[‡][Marchi et al. \(2016\)](#)

Table 3. The probability of forming basins with $D_{crat} > 400$ km, obtained from our model production function for Vesta using the Poisson statistics. The early instability is assumed here, and no crater erasure is accounted for.

Isochrone (Ga)	μ	$p_{\mu}(1)$	$p_{\mu}(2)$
$T < 1.0$	0.16	13%	1%
$T < 2.0$	0.28	21%	3%
$T < 3.0$	0.40	27%	5%
$T < 4.56$	0.65	34%	11%

Table 4. The probability of forming Rheasilvia and Venenia basins ($D_{crat} > 400$ km), assuming that the former formed at $T \leq 1$ Ga and considering different age intervals for the later.

Venia Age (Ga)	Early Instability	Late Instability
$1.0 < T < 4.56$	6.0%	4.0%
$1.0 < T < 3.0$	2.0%	1.0%
$1.0 < T < 2.0$	1.5%	0.0%

Figure 1. A comparison of model impact chronologies for Ceres (blue line), Vesta (red line) and the Moon (black line). In panel (a), the chronology functions were normalized to one asteroid remaining in the main belt today. The solid lines are the chronologies for the instability time $T_{\text{inst}} = 4.5$ Ga and the dashed lines are the chronologies for $T_{\text{inst}} = 3.9$ Ga. In (b), the functions are absolutely calibrated to $\mathcal{N}(> 9 \text{ km}) \simeq 10\,500$ main belt asteroids. The shaded area in (b) represents Vesta’s chronologies obtained in O’Brien et al. (2014), assuming $f_{\text{sl}} = 8$ (the upper boundary) and $f_{\text{sl}} = 20$ (the lower boundary).

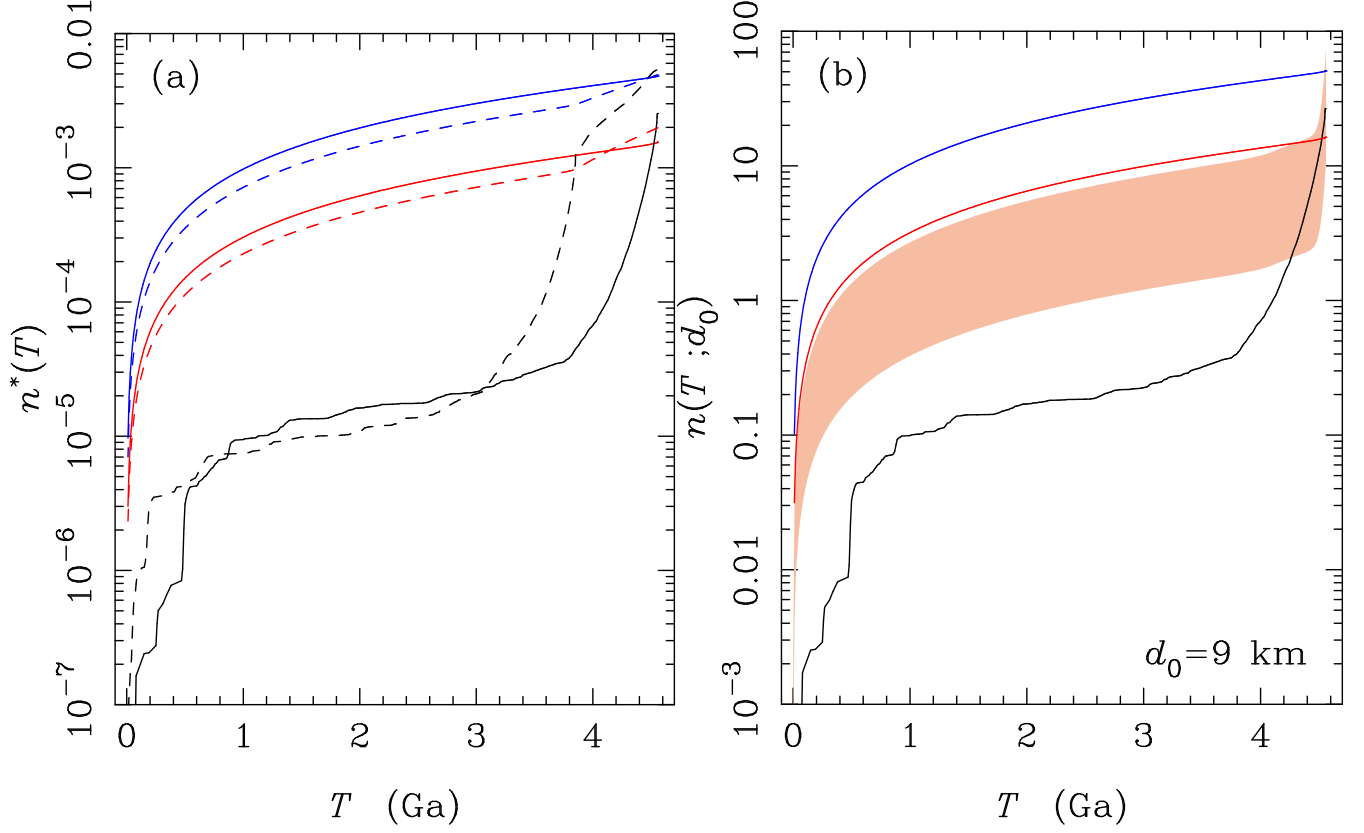


Figure 2. The simulated (solid lines) and observed (red dots) cumulative size distribution of Vesta’s craters. The dashed lines are the 1σ uncertainties of model distributions obtained from 1000 trials with the Monte Carlo method described in Sect. 2.3. In each trial, we generate a number n of impacts of main belt asteroids, where n is drawn from a Poisson distribution with mean $\bar{n} = 47$. This corresponds to the expected number of impacts of asteroids with $D_{\text{ast}} \geq 6$ km (families included) over 4.56 Gy. The early instability chronology is used here. The error bars correspond to $\pm\sqrt{N}$, where N is the number of craters identified on the surface (Marchi et al. 2012b). From left to right, the panels show results without crater erasure, with crater erasure, and with crater erasure and assuming that the Rheasilvia basin formed at 1 Ga.

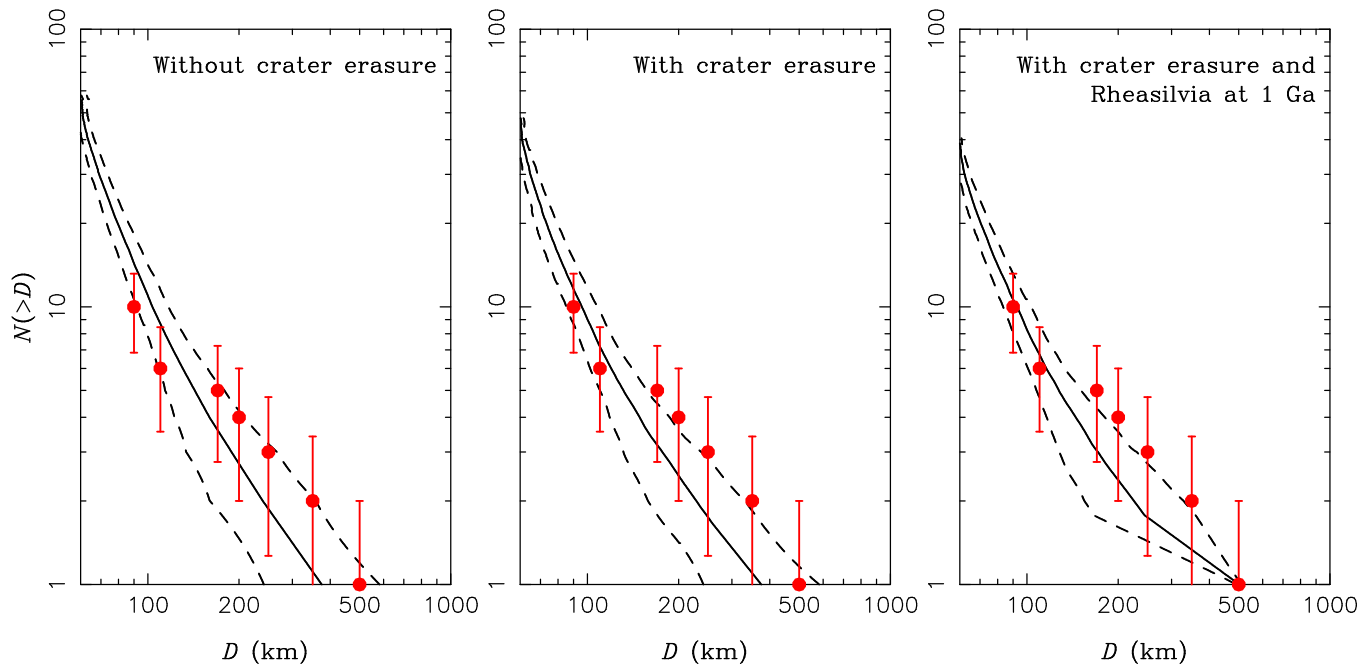


Figure 3. The simulated (solid lines) and observed (blue dots) cumulative size distribution of Ceres’s craters. The dashed lines are the 1σ uncertainties of model distributions obtained from 1000 trials with the Monte Carlo method described in Sect. 2.3. In each trial, we generate a number n of impacts of main belt asteroids, where n is drawn from a Poisson distribution with mean $\bar{n} = 416$. This corresponds to the expected number of impacts of asteroids with $D_{\text{ast}} \geq 4$ km (families included) over 4.56 Gy. The early instability chronology is used here. The error bars correspond to $\pm\sqrt{N}$, where N is the number of craters identified on the surface (Marchi et al. 2012b). From left to right, the panels show results without crater erasure, with crater erasure, and with crater erasure and viscous relaxation. The Vendimia *planitia* is shown here as a possible impact basin with $D_{\text{crat}} \simeq 800$ km.

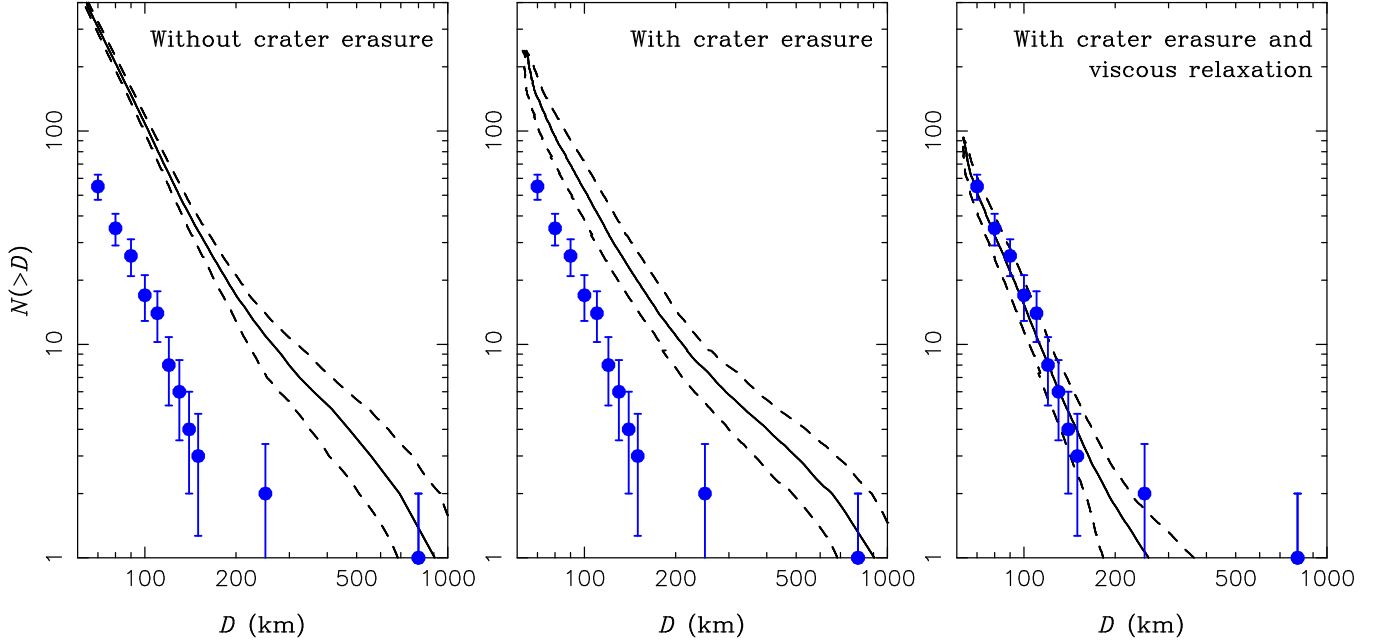


Figure 4. The isochrones derived from our model production function for Vesta in panel (a), and Ceres in panel (b). Each line corresponds to a different age T . The production function for Vesta considers impactors with $D_{\text{ast}} \geq 6$ km, while for Ceres it considers impactors with $D_{\text{ast}} \geq 4$ km, in an early instability model. No crater erasure is used or accounted for in these plots.

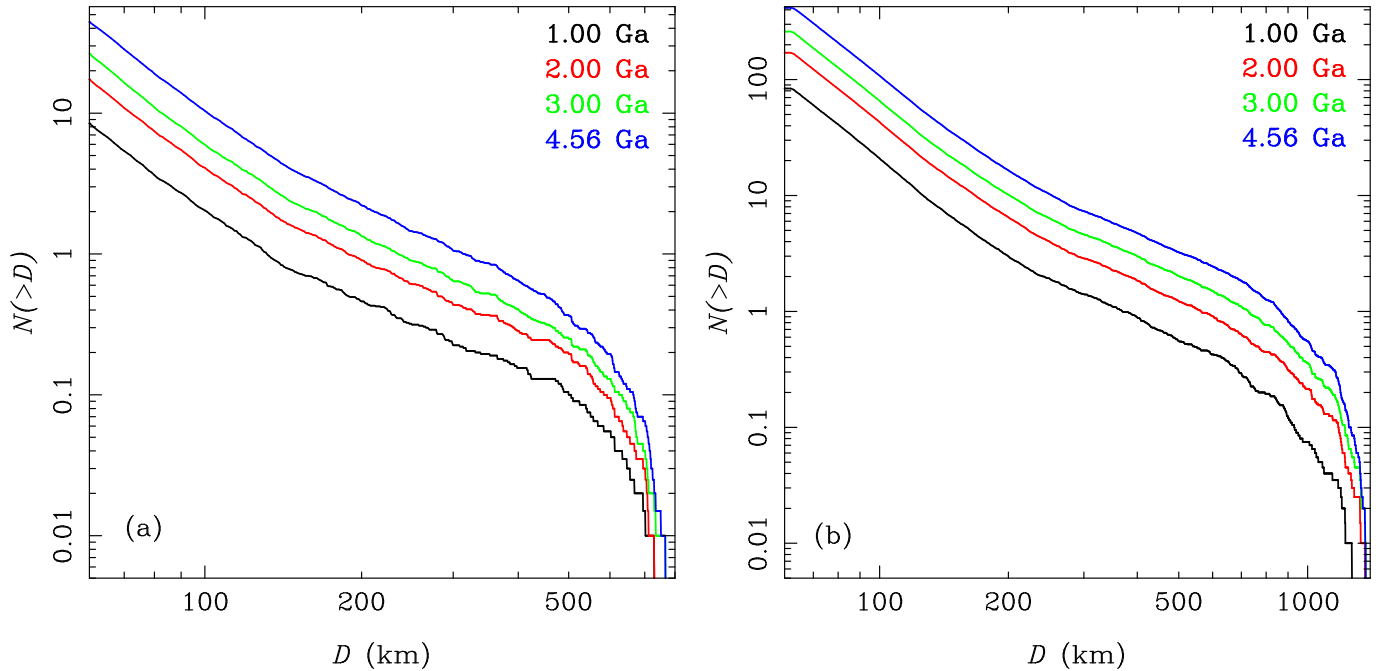


Figure 5. The probability of forming Vesta craters/basins at different times during the solar system history. In panel (a), we plot the probability of creating at least one crater larger than a given size since time T ago. In (b), we plot the probability of creating at least two craters. Each line corresponds to a different cutoff size. The early instability is assumed here, and no crater erasure is included.

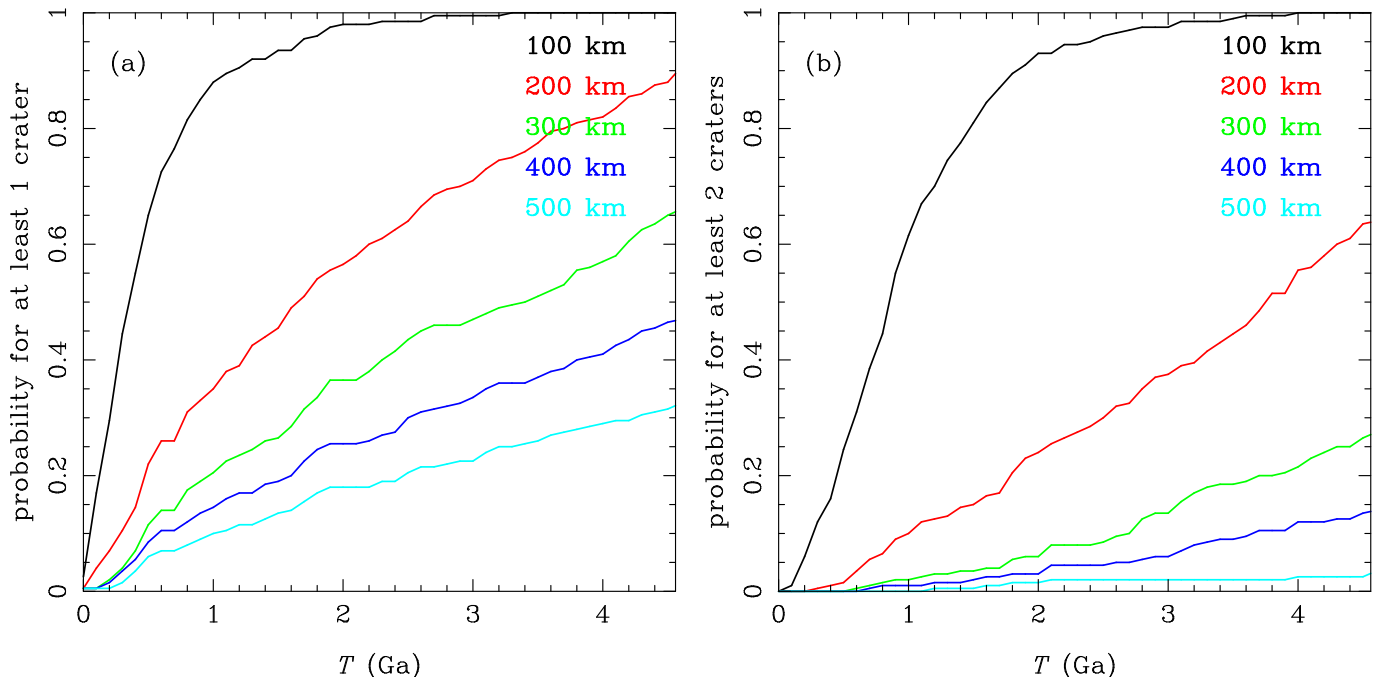


Figure 6. The probability of forming Ceres's craters/basins at different times during the solar system history. The plot shows the probability of creating at least one crater larger than a given size since time T ago. Each line corresponds to a different cutoff size. The early instability is assumed here, and no crater erasure is included.

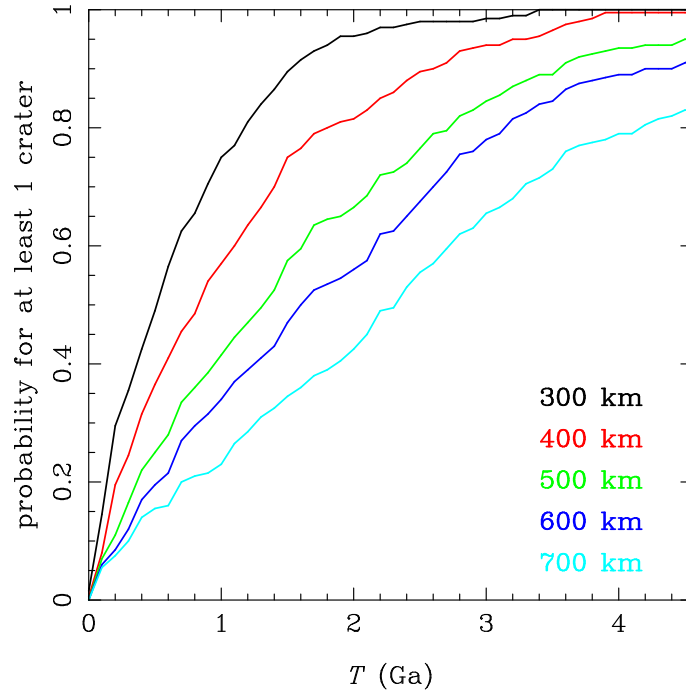


Figure 7. The results of two Monte Carlo simulations of craters with $D_{\text{crat}} > 60$ km on Ceres (left) and Vesta (right). The simulation at the top illustrates a very unlikely case (less than 0.1% of probability) where no large basin formed on Ceres, whereas two basins with $D_{\text{crat}} > 400$ km formed on Vesta. The simulation at the bottom shows a typical outcome of our model, with some very large young basins forming on Ceres. The craters/basins are projected on the surface using the McBryde-Thomas Flat Polar Quartic projection.

